Journal of Applied Mechanics and Technical Physics, Vol. 46, No. 2, pp. 160–167, 2005

NONEQUILIBRIUM MOLECULAR RADIATION BEHIND THE FRONT OF A STRONG SHOCK WAVE IN THE CO_2–N_2–O_2 MIXTURE

V. A. Gorelov, A. Yu. Kireev, and S. V. Shilenkov

UDC 533.6.011

Models of population of some radiating electron-vibrational states of CO, CN*, and* C_2 *molecules are developed. The characteristics of radiation in a chemically nonequilibrium flow behind the front of a strong shock wave in a mixture of gases constituting the Martian atmosphere are calculated. The numerical data are compared with experimental results.*

Key words: *shock wave, nonequilibrium, physicochemical models, ionization, radiation.*

Introduction. The paper describes some results of studying the role of nonequilibrium physicochemical processes in flows behind strong shock waves in complex gas mixtures modeling, in particular, the Martian atmosphere. Results on specific features of ionization processes and preliminary data on chemically nonequilibrium molecular radiation behind a strong shock wave in the Martian atmosphere were previously obtained [1, 2]. Models of formation of nonequilibrium radiation in some molecular systems of bands of the high-temperature CO_2–N_2–O_2 mixture in flows behind the front of a strong shock wave are described in the present paper. The calculation results are compared with the data of laboratory experiments.

Description of the Model. For spacecraft velocities in the Martian atmosphere V_∞ = 4–8 km/sec, the main contribution to the nonequilibrium radiation flux to the frontal surface is made by radiation in bands of CO, CN, and C_2 molecular systems. Modeling of nonequilibrium radiating gas flows is complicated by the lack of reliable data on the kinetics of physicochemical transformations in high-temperature gas mixtures. Based on the analysis of experimental results obtained in the electric-discharge tunnel located at the Central Aerohydrodynamic Institute, some kinetic schemes were proposed in [1], which offer an adequate description of nonequilibrium processes in gas mixtures whose composition simulates the Martian atmosphere. These kinetic schemes are also used in the present work to develop models of chemically nonequilibrium molecular radiation behind the front of a strong shock wave in the CO_2–N_2–O_2 mixture.

We consider the multitemperature model of vibrational relaxation (i.e., vibrational relaxation of CO_2, CO, NO, N_2, CN, and C_2 molecules is characterized by vibrational temperatures T_{V_i}, specific for each molecule and different from the temperature of translational degrees of freedom T). We use Kuznetsov's model to describe the vibrational-dissociation interaction (VDI) of the CO_2 molecule and Treanor and Marrone's CVDV model ($U = D/3$) for diatomic molecules. Dissociation and ionization, as well as exchange reactions and charge-exchange reactions are taken into account. The vibrational relaxation times and the reaction-rate constants used in the numerical model are discussed in detail in [2].

To calculate the characteristics of nonequilibrium molecular radiation, one has to know the populations of the electron-vibrational excited states of molecules responsible for generation of radiation in molecular band systems. The populations of the electron states of molecules, determining radiation in examined molecular band systems, are found by solving the balance equations that take into account formation of excited levels in the course of direct and

Joukowski Central Aerohydrodynamic Institute, Zhukovskii 140180; vgor@tsagi.ru; a_kireev1950@mail.ru; shilenkov@mail.ru. Translated from Prikladnaya Mekhanika i Tekhnicheskaya Fizika, Vol. 46, No. 2, pp. 13–22, March–April, 2005. Original article submitted December 25, 2003; revision submitted June 1, 2004.

stepwise processes of excitation by heavy particles and electrons, resonance processes of energy exchange between the excited states of molecules and molecules in the ground electron state, and radiative depopulation of the state.

It is also assumed in the calculations that the distribution of populations of electron-excited states of molecules over vibrational levels is the Boltzmann distribution with a temperature corresponding to the vibrational temperature of the ground electron state. Rotational temperature of the molecules is assumed to be equal to translational temperature.

The rate constants of reactions with participation of electrons depend on the electron temperature T_e. In the calculations, the electron temperature is assumed to be different from translational and vibrational temperatures and is determined from the equation of the electron-gas energy balance:

$$\frac{d}{dt}\Big(\frac{3}{2}\,T_e n_e\Big) = U_{a.i} + U_{el} + U_{e-R} + \sum_{i=1}^{2} U_{e-v}.$$

This equation takes into account the following processes of energy exchange between electrons and plasma atoms and molecules:

— Origination of electrons with an energy of the order of kT in reactions of associative ionization and the loss of energy in reactions of dissociative recombination of the electron and molecular ion

$$U_{a.i} = \frac{3}{2}\sum_{j=1}^{3}(TR_{f\,j} - T_e R_{r\,j})$$

($R_{f\,j}$ and $R_{r\,j}$ are the rates of the direct and reverse reactions of associative ionization);

— Energy exchange in elastic collisions with atoms and molecules of the mixture

$$U_{el} = \sum_i \frac{3m_e}{m_i}\,\nu_{ei} n_e (T - T_e),$$

where ν_{ei} is the frequency of elastic collisions; m_e and m_i are the masses of the electron and ith heavy particle, respectively;

— Inelastic excitation of rotational degrees of freedom of molecules by an electron impact

$$U_{e-R} = \sum_{j=1}^{6} \frac{64}{\sqrt{3}}\,B_j\Big(\frac{8kT_e}{\pi m_e}\Big)^{05}\sigma_R\Big(\frac{T}{T_e} - 1\Big)n_j n_e,$$

where k is the Boltzmann constant, $\sigma_R = 2\pi s_j^2/(15ea_0^2)$ is the process cross section, s_j is the quadrupole moment of the molecule, and B_j is the rotational constant of the molecule of the jth kind (N_2, O_2, NO, CO, CN, or C_2);

— Inelastic resonant excitation of vibrational levels of the ground electron state of N_2 and CO molecules by an electron impact in the reactions

$$N_2(v) + e = N_2^- = N_2(v') + e; \qquad CO(v) + e = CO^- = CO(v') + e.$$

Here v and v' are the numbers of vibrational levels of the ground electron state of the molecule ($v, v' = 0, \ldots, 8$, $v \neq v'$). For the N_2 molecule, the rate of variation of the electron energy is described by the relation

$$U_{e-V,N_2} = \frac{n_e n_{N_2}}{q}\sum_v v\theta_{N_2}\Big[\exp\Big(-\frac{v\theta_{N_2}}{T_e}\Big)\sum_{v'} k_{vv'}(T_e)\exp\Big(\frac{v'\theta_{N_2}(T_{v,N_2} - T_e)}{T_{v,N_2}T_e}\Big) - \exp\Big(-\frac{v\theta_{N_2}}{T_{v,N_2}}\Big)\sum_{v'} k_{vv'}(T_e)\Big],$$

where q is the vibrational statistical sum for N_2, θ_{N_2} is the characteristic vibrational temperature of the molecule, and $k_{vv'}(T_e)$ is the reaction-rate constant ($v < v'$). For carbon monoxide, the relation is similar (the subscript is changed to CO).

Some constants of reactions of resonant excitation of vibrations in nitrogen and carbon monoxide by an electron impact, which are used in the present work, are listed (in the Arrhenius form) in Tables 1 and 2, respectively. These data are the Arrhenius-form approximation of the reaction-rate constants calculated by the model proposed in [3] with the use of experimentally measured cross sections of the processes [4]:

$$k_{vv'}(T_e) = AT_e^n \exp(-C/T_e)$$

(A is expressed in 10^{-10} cm^3/sec and T_e in eV).

TABLE 1

v	v'	A	n	C
0	1	83	−0.5	1.7
0	2	63	−1.1	1.9
1	2	116	−1.3	2.0
0	3	58	−1.5	2.3
1	3	169	−1.4	2.0
2	3	35	−1.0	1.5
0	4	49	−1.5	2.4
1	4	147	−1.5	2.1
2	4	24	−1.0	1.4
3	4	54	−1.2	1.3

TABLE 2

v	v'	A	n	C
0	1	1144	−1.35	2.63
0	2	447	−1.34	2.97
1	2	208	−2.38	3.54
0	3	42.6	0	1.55
1	3	23.4	−1.17	2.24
2	3	7.6	−1.44	1.6
0	4	245	−2.17	3.6
1	4	17.9	−1.66	2.4
2	4	2.49	−0.8	1.2
3	4	2.28	−1.45	1.5

The resonant processes of excitation of vibrational levels of nitrogen and carbon monoxide by an electron impact determine (under conditions of weak dissociation of N_2 and CO) the behavior of the electron temperature T_e in the relaxation zone. The calculated distribution of T_e is plotted in Fig. 1. The maximum value of the electron temperature on the wave front is close to the translational temperature T. Because of the strong energy exchange between electrons and molecular vibrations, T_e relaxes to vibrational temperatures of N_2 or CO (depending on N_2 and CO concentrations and flow temperatures).

Radiation of CO(4+). Molecular radiation in the CO(4+) band system is formed in the transition CO($A^1\Pi \rightarrow X^1\Sigma$). The state CO($A^1\Pi$) ≡ CO(A) is populated (depopulated) in the course of the basic reactions listed in Table 3.

Radiation of CN(violet). Molecular radiation in the CN(violet) band system is formed in the transition CN($B^2\Sigma^+ \rightarrow X^2\Sigma^+$). The state CN($B^2\Sigma^+$) ≡ CN(B) is populated (depopulated) in the course of the basic reactions listed in Table 4.

Radiation of C_2(Swan). Molecular radiation in the C_2(Swan) band system is formed in the transition $C_2(d^3\Pi_g \rightarrow a^3\Pi_u)$. The state $C_2(d^3\Pi_g) \equiv C_2(d)$ is populated (depopulated) in the course of the basic reactions listed in Table 5.

The rate constants and reactions leading to population (depopulation) of the electron-excited states of CO, CN, and C_2 molecules, listed in Tables 3–5, were chosen from a numerical experiment performed on the basis of scarce published data (see, e.g., [5–10]) and a subsequent comparison with the measurement results obtained at Central Aerohydrodynamic Institute. The cross sections of the resonant processes of energy exchange between metastable and short-lived states of the molecules were estimated on the basis of the model developed in [8]. The lifetimes of optical transitions used in the calculations were borrowed from the monograph [10].

Figures 2 and 3 show the gradients of concentrations $(dc/dx)_j$ of excited CO(A) (Fig. 2) and CN(B) (Fig. 3) molecules formed in reactions (reaction numbers are given in Tables 3 and 4) versus the distance in the relaxation zone behind the shock-wave front (c is the mass concentration of electron-excited molecules and x is the distance behind the wave front). The positive and negative values of $(dc/dx)_j$ indicate the population and depopulation of the excited level in the jth reaction, respectively.

The data shown in Figs. 2 and 3 were obtained for the shock-wave velocity $V_s = 6$ km/sec and initial pressure $P_1 = 0.2$ torr. One can easily see that the main contribution to population of the electron-excited state of CO($A^1\Pi$) under these conditions is made by reaction No. 1 [excitation from the metastable state of CO(a)] and No. 4 (direct excitation by heavy particles). Reaction No. 6 leads to radiative depopulation of the state. Other reactions contribute insignificantly in this flow regime. Figure 3 illustrates the importance of taking into account the resonant processes of CN($B^2\Sigma^+$) formation (reaction Nos. 1 and 2), which, together with reactions of direct population by heavy particles (reaction No. 3) and radiative depopulation of the state (reaction Nos. 5 and 6), determine the electron-excited state population.

Verification of Radiation Kinetics. The specific features of nonequilibrium radiation in a gas mixture simulating the Martian atmosphere was experimentally modeled in the electric-discharge tunnel located at Central Aerohydrodynamic Institute. Some features of the tunnel structure, its operation parameters, and the experimental technique are described in [1, 11]. The length and diameter of the low-pressure channel are 5 m and 57 mm, respectively. The major part of experiments were performed with a gas mixture modeling the composition of the Martian atmosphere and containing 96% CO_2, 3% N_2, and 1% O_2, the initial pressure in the channel being

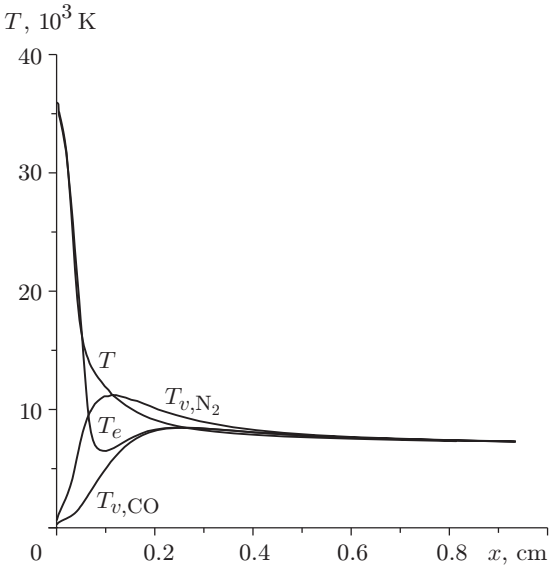

Fig. 1. Translational (T), vibrational ($T_{v,\mathrm{N_2}}$ and $T_{v,\mathrm{CO}}$), and electron (T_e) temperatures behind the shock-wave front for a 97% CO_2 + 3% N_2 mixture ($V_s = 7$ km/sec and $P_1 = 0.2$ torr).

TABLE 3

Reaction	$k_f = AT^B \exp(-C/T)$ [cm^3/mole · sec] or τ [sec]		
	A	B	C
1. CO(a) + M = CO(A) + M	$2.00 \cdot 10^{13}$	0	23,000
2. CO(a) + e = CO(A) + e	$4.00 \cdot 10^{15}$	0	23,000
3. N_2(A) + CO(X) = CO(A) + N_2	$1.10 \cdot 10^{10}$	0	21,600
4. CO(X) + M = CO(A) + M	$4.50 \cdot 10^{2}$	2.86	93,000
5. CO(X) + e = CO(A) + e	$4.00 \cdot 10^{11}$	0.93	93,000
6. CO(A) → CO(X) + $h\nu$	$\tau = 3.03 \cdot 10^{-8}$		

TABLE 4

Reaction	$k_f = AT^B \exp(-C/T)$ [cm^3/mole · sec] or τ [sec]		
	A	B	C
1. CN(X) + CO(X, $v > 12$) = CN(B) + CO(X)	$6.00 \cdot 10^{13}$	0	0
2. CN(X) + N_2(X, $v > 11$) = CN(B) + N_2	$6.00 \cdot 10^{13}$	0	0
3. CN(X) + M = CN(B) + M	$2.24 \cdot 10^{10}$	0.5	37,000
4. CN(X) + e = CN(B) + e	$7.80 \cdot 10^{13}$	0.5	37,000
5. CN(B) → CN(X) + $h\nu$ CN(B) → CN(A) + $h\nu$	$\tau = 6.55 \cdot 10^{-8}$		

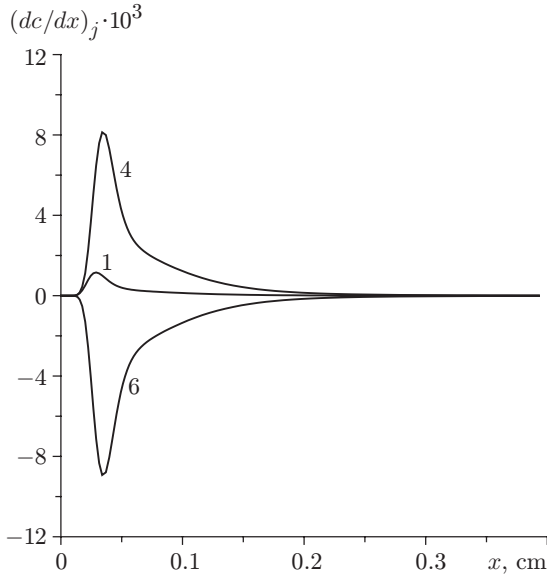

Fig. 2

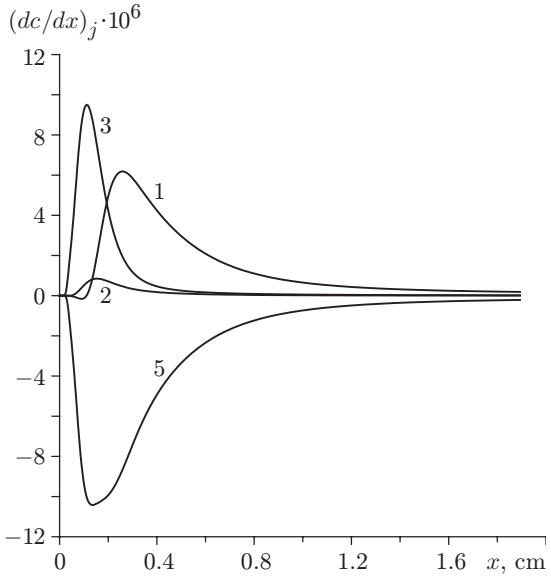

Fig. 3

Fig. 2. Distribution of concentration gradients $(dc/dx)_j$ of the electron-excited CO($A^1\Pi$) molecule formed in reaction Nos. 1, 4, and 6 (see Table 3) for a 97% CO_2+3% N_2 mixture ($V_s = 6$ km/sec and $P_1 = 0.2$ torr).

Fig. 3. Distribution of concentration gradients $(dc/dx)_j$ of the electron-excited CN($B^2\Sigma^+$) molecule formed in reaction Nos. 1, 2, 3, and 5 (see Table 4) for a 97% CO_2 + 3% N_2 mixture ($V_s = 6$ km/sec and $P_1 = 0.2$ torr).

TABLE 5

Reaction	$k_f = AT^B \exp(-C/T)$ [cm^3/mole · sec] or τ [sec]		
	A	B	C
1. $C_2(X) + M = C_2(d) + M$	$2.90 \cdot 10^{14}$	0.15	28,807
2. $C_2(X) + e = C_2(d) + e$	$7.80 \cdot 10^{15}$	0.15	28,807
3. $C_2(d) \rightarrow C_2(a) + h\nu$	$\tau = 3.57 \cdot 10^{-8}$		

$P_1 = 0.2$ torr (±1%). The shock-wave velocity in the channel was measured within 2%. The residence time of the gas flow compressed by the shock wave in the channel cross section where the radiation was registered was 7–3 μsec for the shock-wave velocity of 4–9 km/sec. The optical system allowed registration of gas radiation in the direction perpendicular to the shock-tunnel channel axis with a spatial resolution of 0.1 mm along the channel centerline. The spectral studies were performed by the conventional technique with the use of a multichannel spectrometer and a monochromator. Radiation detectors were photomultipliers. The signals of photomultipliers were registered by a digital oscillograph with a resolution of 0.1 μsec.

Nonequilibrium Radiation of CN(violet). The experimental and numerical data on nonequilibrium radiation in the CN(violet) molecular system in the range of shock-wave velocities $V_s = 5.5$–9 km/sec are compared in [1]. The numerical and experimental data on intensities of nonequilibrium radiation in the CN system and on the dependence of the nonequilibrium radiation maximum on the shock-wave velocity in the considered range of its variation are in good agreement. The numerical data were also compared with the experimental results of [12]. Figure 4 shows a comparison of the calculated spectrum of integral radiation (integrated over the length of the relaxation zone to the distance $x = 10$ cm) with the results measured in [12] on intensity of integral nonequilibrium radiation of the CN(violet) band system behind the front of a strong shock wave. Figure 4 displays good agreement between numerical and experimental data.

Nonequilibrium Radiation of CO(4+). Nonequilibrium radiation in the CO(4+) molecular system makes the basic contribution to nonequilibrium radiation of the gas behind the shock-wave front. Unfortunately, available instrumentation did not allow experimental measurements of nonequilibrium radiation in the spectral range

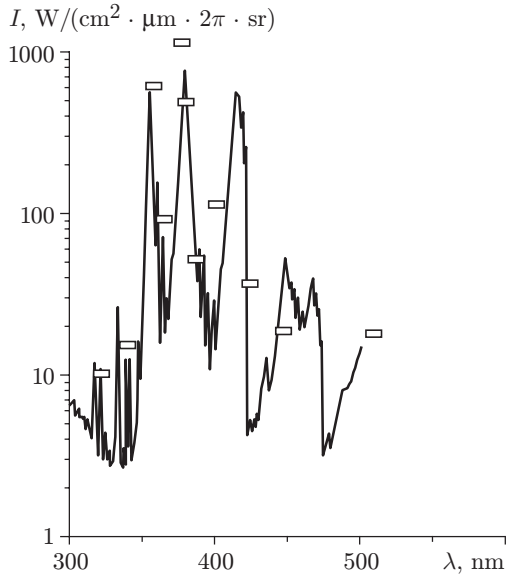

Fig. 4

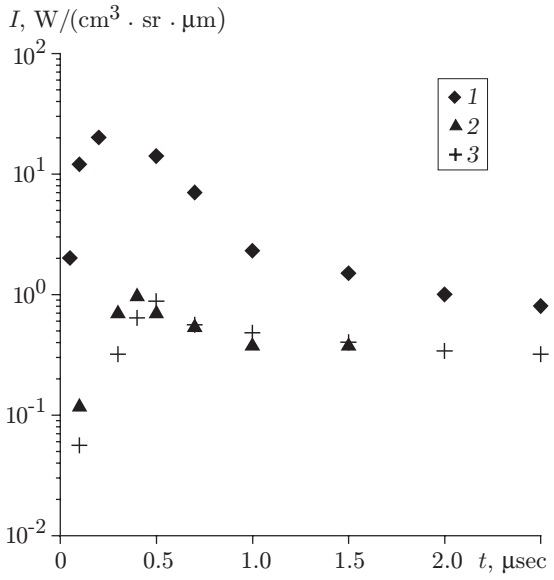

Fig. 5

Fig. 4. Spectrum of nonequilibrium integral radiation of CN(violet) behind the shock-wave front for a 30% CO_2 + 70% N_2 mixture (V_s = 7.62 km/sec and P_1 = 0.25 torr): the curve refers to the calculated data and the points refer to the measurements of [12].

Fig. 5. Measured distributions of nonequilibrium radiation intensity behind the shock-wave front for V_s = 7.3 km/sec and P_1 = 0.2 torr: points 1 refer to CO(4+), points 2 to CN(violet), and points 3 to C_2(Swan).

corresponding to the radiation maximum in the CO(4+) system (λ = 150 μm). Therefore, the numerical and experimental results were compared in the spectral range $\lambda = (200 \pm 3.4)$ nm. Figure 5 shows the profiles of nonequilibrium radiation measured in the spectral ranges (200 ± 3.4) nm [for CO(4+)], (388 ± 1.3) nm [for CN(violet)], and (515 ± 1.3) nm [for C_2(Swan)]. The time t corresponds to arrival of the shock wave in the cross section where the radiation was measured. In addition to a large difference in intensity of nonequilibrium radiation in CO(4+), CN, and C_2 systems, there is a difference in times when the maximum radiation values are reached in the CO(4+) system and in the CN and C_2 systems.

Figure 6 shows the time characteristics of the nonequilibrium radiation peak ($t_{\max}$ is the time when the radiation maximum is reached and t_{qs} is the characteristic duration of the nonequilibrium radiation peak) for radiation in the CO(4+) system at λ = 200 nm and for radiation in the CN(violet) system, which were measured in experiments performed in electric-discharge tunnel at Central Aerohydrodynamic Institute. The same figure shows the results of similar measurements performed in [12] and also the results of numerical calculations of $t_{\max}$ and t_{qs} for CN radiation. The measured values of $t_{\max}$ and t_{qs} for the CN system agree with the data of [12] obtained for the 30% CO_2 + 70% N_2 mixture and with numerical results. Yet, the calculated time characteristics of the peak of nonequilibrium radiation of the CO(4+) system differ from the measured values. The times $t_{\max}$ are very small (0.1–0.2 μsec) and lie within the uncertainty band determined by the discrete system of signal registration (0.1 μsec). The duration of the peak of nonequilibrium radiation in the CO(4+) system is also very small. There is a maximum in the dependence of the time t_{qs} on the shock-wave velocity at $V_s \approx$ 7–8 km/sec. Note, the characteristic growth time of 0.1 μsec corresponds to the distance $x \approx 3\lambda_\infty$, where λ_∞ is the mean free path of molecules upstream of the shock-wave front. Hence, the maximum generation of CO(4+) radiation can occur in the zone of the shock-wave "structure" with the so-called thermal nonequilibrium. Therefore, the model of a straight shock wave (without allowance for high-energy collisions in the wave-front zone) can underpredict the intensity of nonequilibrium radiation in the CO(4+) system.

Figure 7 shows the peak radiation intensity in the CO(4+) system, which was registered in experiments in electric-discharge tunnel, as a function of velocity V_s and the corresponding calculations based on the above-

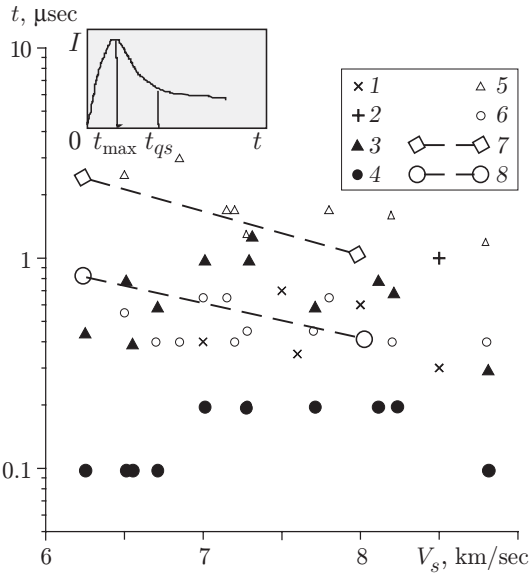

Fig. 6. Measured and calculated dependences of the time characteristics of nonequilibrium radiation in CO(4+) and CN(violet) systems behind the shock-wave front on the wave velocity for $P_1 = 0.2$ torr: points 1 and 2 refer to the measurements of [12] for $t_{\max}$ of CN(violet) (1) and t_{qs} of CN(violet) (2); points 3–6 refer to the measurements of the present work for t_{qs} of CO(4+) (3), $t_{\max}$ of CO(4+) (4), t_{qs} of CN(violet) (5), and $t_{\max}$ of CN(violet) (6); curves 7 and 8 refer to the calculations for t_{qs} of CN(violet) and $t_{\max}$ of CN(violet), respectively.

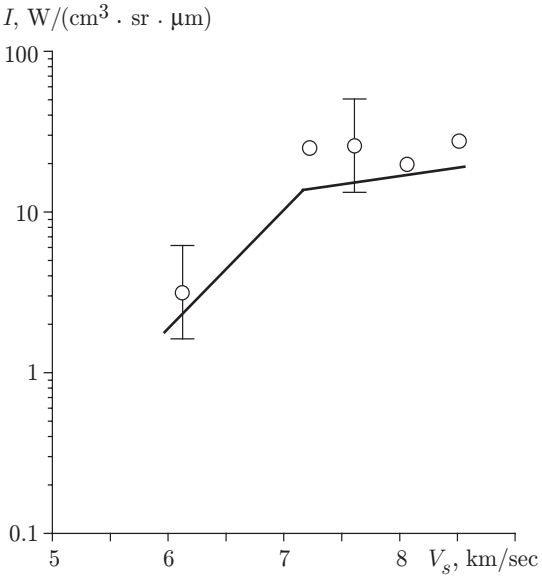

Fig. 7

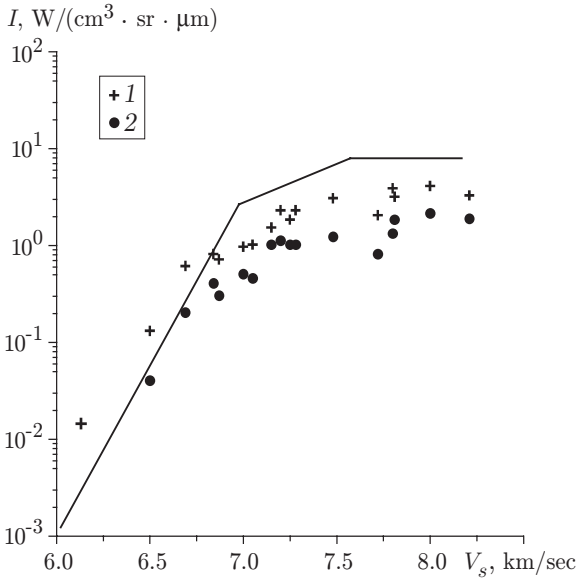

Fig. 8

Fig. 7. Peak values of the flux of radiant energy of CO(4+) behind the shock-wave front versus the wave velocity for $P_1 = 0.2$ torr: the curve and the points show the calculated and experimental data, respectively.

Fig. 8. Maximum and quasi-steady values of radiation intensity in the C_2(Swan) system behind the shock-wave front versus the wave velocity for $P_1 = 0.2$ torr: the curve shows the calculated values of $I_{\max}$; the points show the experimentally measured values of $I_{\max}$ (1) and I_{qs} (2).

described kinetics of radiation in the model with a straight shock wave. It is seen that the calculations underpredict the maximum of the nonequilibrium peak.

Nonequilibrium Radiation of C_2(Swan). The numerical calculations of the maximum intensity of nonequilibrium radiation in the C_2(Swan) molecular system ($\lambda \approx 585$ nm) versus the velocity of the straight shock wave ($V_s = 6$–8 km/sec) are compared with the experimental data obtained in electric-discharge tunnel in Fig. 8. The simplified model of nonequilibrium radiation of C_2 (see Table 5) does not provide good agreement with the experiment for $V_s \geqslant 7$ km/sec. Additional investigations of the kinetics of formation and excitation of the C_2 molecule under the conditions considered are needed. Nevertheless, because of a comparatively small contribution of C_2 radiation to the total intensity of radiation behind the shock wave in the Martian atmosphere [1, 8], the present stage of research did not involve improvement of C_2 radiation kinetics.

Conclusions. The numerical model of physicochemical processes, which was developed and compared with the results of tunnel experiments, and the models of radiation generation in some electron-vibrational transitions of CO, CN, and C_2 molecules behind strong shock waves in the CO_2–N_2–O_2 mixture can be used to determine the characteristics of nonequilibrium molecular radiation in estimating the radiant flux to the surface of a space vehicle on its landing trajectory in the Martian atmosphere with velocities of 4–8 km/sec.

The authors are grateful to S. T. Surzhikov (Institute of Problems in Mechanics, Russian Academy of Sciences) and L. A. Kuznetsov (Chemical Department of the Lomonosov Moscow State University) for advanced spectroscopic data and to L. A. Kil'dyushov (Central Aerohydrodynamic Institute) for his assistance in processing experimental results.

This work was supported by the Russian Foundation for Basic Research (Grant Nos. 01-01-00467 and 04-01-00551).

REFERENCES

1. V. A. Gorelov, M. K. Gladyshev, A. Yu. Kireev, et al., "Nonequilibrium ionization and radiation behind shock wave in Martian atmosphere," in: *Proc. of the 3th Europ. Symp. on Aerothermodynamics for Space Vehicles* (Noordwijk, Netherlands, November 24–26, 1998), ESTEC, Noordwijk (1998), pp. 429–436.
2. V. A. Gorelov, M. K. Gladyshev, A. Yu. Kireev, and S. V. Shilenkov, "Nonequilibrium ionization behind a strong shock wave in the Mars atmosphere," *J. Appl. Mech. Tech. Phys.*, **41**, No. 6, 970–977 (2000).
3. A. A. Mikhailov and V. A. Pivovar, "Model calculation of rate constants of stepwise excitation of vibrational levels of nitrogen by an electron impact," *Zh. Tekh. Fiz.*, **45**, No. 5, 1063–1068 (1975).
4. G. J. Schultz, "Vibrational excitation of N_2, CO and H_2 by electron impact," *Phys. Rev.*, **135**, No. 4A, 531–536 (1966).
5. V. A. Gorelov, M. K. Gladyshev, A. Yu. Kireev, et al., "Experimental and numerical study of nonequilibrium ultraviolet NO and N_2^+ emission in shock layer," *J. Thermophys. Heat Transfer*, **12**, No. 2, 172–180 (1998).
6. N. E. Afonina and V. G. Gromov, "Numerical modeling of the flow around a Martian lander," *Aéromekh. Gaz. Dinam.*, No. 2, 35–47 (2001).
7. N. N. Kudryavtsev, L. A. Kuznetsova, and S. T. Surzhikov, "Kinetics and nonequilibrium radiation of CO_2–N_2 shock waves," AIAA Paper No. 2001-2728 (2001).
8. J. A. Drakes, W. K. McGregor, and A. A. Mason, "Two-electron exchange in collisions of neutral molecules," *J. Chem. Phys.*, **99**, No. 10, 7813–7818 (1993).
9. S. A. Losev et al., "Radiation of a mixture CO_2–N_2–Ar in shock waves: experiment and modelling," in: *Proc. of the 3rd Europ. Symp. on Aerothermodynamics for Space Vehicles* (Noordwijk Netherlands), 24–26 November, 1998), ESA/ESTEC SP-426 (1998), pp. 438–444.
10. L. A. Kuznetsova, N. E. Kuz'menko, Yu. A. Kuzyakov, and Yu. A. Plastinin, *Probability of Optical Transitions of Diatomic Molecules* [in Russian], Nauka, Moscow (1980).
11. V. A. Gorelov, L. A. Kildushova, and A. Yu. Kireev, "Ionization particularities behind intensive shock waves in air at velocities of 8–15 km/sec," AIAA Paper No. 94-2051 (1994).
12. G. M. Thomas and W. A. Menard, "Experimental measurements of nonequilibrium and equilibrium radiation from planetary atmospheres," *AIAA J.*, **4**, No. 2, 227–237 (1966).